Electrical Resistivity Tensor for Aluminum Single Crystals Deformed at Helium Temperature*

A. SOSIN AND J. S. KOEHLER
University of Illinois, Urbana, Illinois

(Received February 11, 1955; revised manuscript received November 14, 1955)

Stress-strain curves and electrical resistance measurements were made on single crystals of 99.99+% pure aluminum pulled in tension at 4°K. The stress-strain data show that beyond the easy-glide region the stress-strain curves are linear with a slope that depends on crystal orientation. If the specimen is unloaded and aged at room temperature, a small upper yield point occurs on reloading at 78°K or 4°K. The resistance produced by deformation is the same in all crystallographic directions. It increases as the square of the resolved shearing stress. Annealing at 78°K produces a 10% drop in the strain-induced resistivity (which is still isotropic). Annealing at 300°K produces a 65% drop in the strain-induced resistivity (again isotropic).

1. INTRODUCTION

A DEFORMED single crystal probably contains lattice vancancies, interstitial atoms, dislocations, and stacking faults. In the present experiments, an attempt was made first, to secure a simple type of deformation by making tensile tests at helium temperature; and second, to analyze the types and amounts of defect present by measuring all components of the resistivity tensor. The measurements were made at helium temperature on deformation and subsequently after various annealing treatments.

2. EXPERIMENTAL PROCEDURES

The experiment has been performed on single crystals of high-purity (99.99+%) aluminum at liquid helium and nitrogen temperatures. Aluminum was used because Dexter[1] and later workers have calculated the electrical resistance changes produced by dislocations in an elastically isotropic medium; aluminum is very nearly elastically isotropic.

The preparation of samples followed a technique developed by Noggle.[2] In brief, the method is an elaboration of the Bridgman technique of growing single crystals which allows one to obtain a specimen arbitrarily shaped by using a "soft" mold to contain the molten metal. The specimen is shown in Fig. 1 as it would appear prior to melting. The sixteen potential leads indicated are cast in place. They are located on the central gauge length of reduced section, $\frac{1}{2}$ centimeter apart axially and 90° apart around the circular cross section. As indicated, the diameter of the gauge length is approximately 0.350 in. This relatively large dimension was necessary to attain the accuracy of geometry in making anisotropy measurements. A detailed machining procedure was followed in locating potential probes. The probes were drawn from the original pure aluminum stock to 0.014-in. diameter. Their positions were carefully located using a Tukon hardness indenter with a traveling stage microscope. This was followed by drilling 0.0135-in. diameter holes approximately $\frac{1}{8}$ in. deep centered by the indentations. Finally, the aluminum wire was inserted.

The crystals were deformed in tension using a tensile machine designed and built in this laboratory. Maximum available load was greater than 1000 pounds. To allow free rotation of the specimen during loading, gimble and universal joints were included in the pulling system. Load and head motion (extension) were read directly by counters geared to the machine.

The pulling system was designed for operations at liquid helium temperature (4°K). Double Dewar flasks were used with liquid nitrogen in the outer flask and a can of liquid nitrogen situated above the helium for complete shielding. The same apparatus served for operations at liquid nitrogen temperature (78°K). With additional control equipment it was possible to extend the investigation over the range from 78°K to room temperature (300°K).

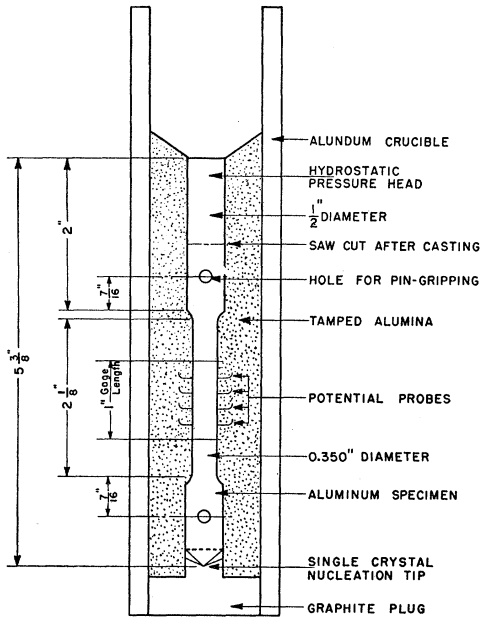

FIG. 1. Section through specimen as grown by Bridgman method in the soft mold.

* This work was supported by the Office of Naval Research and Office of Ordnance Research.

[1] D. L. Dexter, Phys. Rev. 86, 770 (1952).
[2] T. S. Noggle, Rev. Sci. Instr. 24, 184 (1953).

The resistance measurements were made by the *IR*-drop method. That is, a known current of between 15 and 22 amperes was passed axially down the specimen and the drop in voltage between various sets of probes determined. These voltages were less than one microvolt when taken at 4°K. To measure such voltages, a Rubicon thermofree microvolt potentiometer was indispensable.

Six-volt storage batteries were the source of potential. Leakage currents and heating effects were searched for by varying the current level but found to be absent. Total heat dissipation in the specimen and current contacts was less than four milliwatts. To compensate for contact and thermal emf, readings of potential drop were made with the direction of the current reversed. The stray emf calculated by this procedure agreed with the measured no-current potential.

Temperatures were measured by means of two copper-constantan thermocouples placed at the ends of the specimen. Elongations were usually measured by means of a traveling microscope after each strain increment. This is undoubtedly the source of largest experimental error. To minimize this error, readings of electrical resistance were taken before and after each strain increment in an ice bath, whenever possible. Since the residual portion of the resistivity is a negligible portion of the total resistivity at 0°C, the change in electrical resistance at 0°C is an excellent measure of the strain.

TABLE I. Resistivity at 4°K (in 10^{-9} ohm cm) in specimen 31 on deformation and annealing. $\cos(xz')=0.145$.

ϵ	ρ_x	ρ_y	ρ_z	Remarks
1.0	6.78	6.17	6.49	As-grown specimen
1.09	8.22	9.19	9.51	Pulled to 9% elongation at 4°K
1.15	13.80	14.89	13.64	Pulled to 15% elongation at 4°K
1.15	13.03	13.35	12.95	Annealed at 78°K over-night
1.15	8.72	8.78	9.05	Annealed at 300°K for two weeks

TABLE II. Resistivity at 4°K (in 10^{-9} ohm cm) in specimen 33 on deformation and annealing. $\cos(xz')=0.37$.

ϵ	ρ_x	ρ_y	ρ_z	Remarks
1.0	7.10	7.03	7.05	As-grown specimen
1.03	8.01	7.46	7.53	Pulled to 3% elongation at 4°K
1.09	10.62	10.42	10.85	Pulled to 9% elongation at 4°K
1.09	10.79	10.05	10.26	Annealed at 78°K over-night
1.09	8.78	8.10	8.27	Annealed at 300°K for four days
1.13	12.42	11.74	12.02	Pulled further at 4°K

TABLE III. Resistivity at 4°K (in 10^{-9} ohm cm) in specimen 32 on deformation and annealing. $\cos(xz')=0.11$.

ϵ	ρ_x	ρ_y	ρ_z	Remarks
1.0	7.76	7.91	7.68	As-grown specimen
1.16	8.60	13.54	12.96	Pulled to 16% elongation at 78°K
1.16	10.32	9.37	9.17	Annealed to 300°K for three days

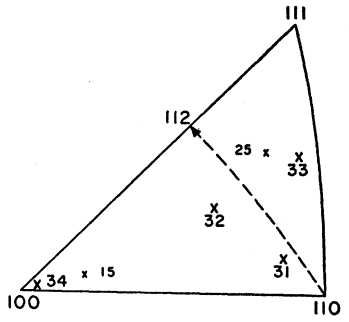

FIG. 2. Initial orientation of the tensile axis for the various aluminum single crystals tested.

3. RESISTIVITY CALCULATIONS

The observations made in connection with a given strain are as follows: (1) the initial orientation of crystal axes relative to specimen axis and potential probes; (2) the initial location of the potential probes; (3) the tensile extension, and the total load; (4) the total current I, and (5) the voltage differences between various potential leads (both at zero extension and after extension).

The above data allow one to calculate the components of resistivity as follows. Since the problem is independent of time, the differential equation to be solved is $\mathrm{div}(\sigma\ \mathrm{grad}\varphi)=0$, where φ is the electrical potential and σ is the electrical conductivity, a second rank tensor. The boundary conditions are that the current density normal to the surface of the specimen vanish and that the integral of the current density across any cross section of the specimen is equal to the total current, I.

Since the experimental runs were made using crystals which deformed in single slip throughout the run, it seems reasonable (as first mentioned by Sondheimer and Mackenzie[3]) to take the principal axes of the conductivity tensor as the slip direction—the y-axis $(1\bar{1}0)$, the normal to the slip plane—the z-axis (111), and the third orthogonal direction—the x-axis $(11\bar{2})$.

The solution to the equation then becomes

$$\Delta\phi=(I/A)[\rho_x\Delta x\cos(xz')+\rho_y\Delta y\cos(yz')+\rho_z\Delta z\cos(zz')],$$

where A is the cross-sectional area of the specimen within the gauge length; ρ_x, ρ_y, ρ_z are the three components of the resistivity tensor referred to the principal axes; Δx, Δy, and Δz are the relative coordinates of the two potential probes under consideration. These coordinates are measured along the principal axes of the resistivity tensor. The direction cosines are of angles between the principal axes and the current direction (i.e., the specimen axis).

The area, A, at any strain level is simply A_0/ϵ, where A_0 is the initial area and ϵ is the ratio of gauge length at the given strain to the original gauge length.

The relative coordinates Δx, Δy, Δz, and the direction cosines can be calculated from the initial dimensions

[3] E. H. Sondheimer and J. K. Mackenzie, Phys. Rev. **77**, 264 (1950).

TABLE IV. The behavior of the average resistivity at 4°K (in 10^{-9} ohm cm) on deformation and annealing.[a]

Specimen	ϵ	ρ_u	ρ_4	ρ_{78}	ρ_{300}	$\frac{\rho_{78}-\rho_4}{\rho_4-\rho_u}$	$\frac{\rho_{300}-\rho_{78}}{\rho_{78}-\rho_u}$	$\frac{\rho_{300}-\rho_{78}}{\rho_4-\rho_u}$
33	1.09	7.05	10.62	10.27	8.35	0.10	0.60	0.54
31	1.15	6.40	14.44	13.20	8.86	0.16	0.64	0.54
32	1.16	7.68	...	13.29	9.32	...	0.72	...

[a] $(\epsilon-1)\times100$ = percent elongation. ρ_u = resistivity of undeformed crystal measured at 4°K. ρ_4 = resistivity of deformed crystal, deformed and measured at 4°K. ρ_{78} = resistivity of deformed crystals measured at 4°K. Specimens 33 and 31 were deformed at 4°K, warmed to 78°K. Specimen 32 was deformed at 78°K. ρ_{300} = resistivity of deformed crystals measured at 4°K after warming to 300°K.

of the specimen, the initial orientation, the initial location of the potential probes, and the tensile strain. The equations obtained by assuming that only one slip system operates are given in Appendix I. The assumption was made that the volume of the material is unchanged during deformation.

4. EXPERIMENTAL RESULTS

The experimental resistivity changes found on deformation and annealings are given in Tables I to IV. Initial orientations are given in Fig. 2. Further results are given in Figs. 3 to 7.

The following results are found for deformation at 4°K.

(1) The changes in resistivity are isotropic to within the accuracy discussed in Appendix II.

(2) The resistivity increases are proportional to the square of the resolved shearing stress (see Blewitt and co-workers[4] for similar results on copper).

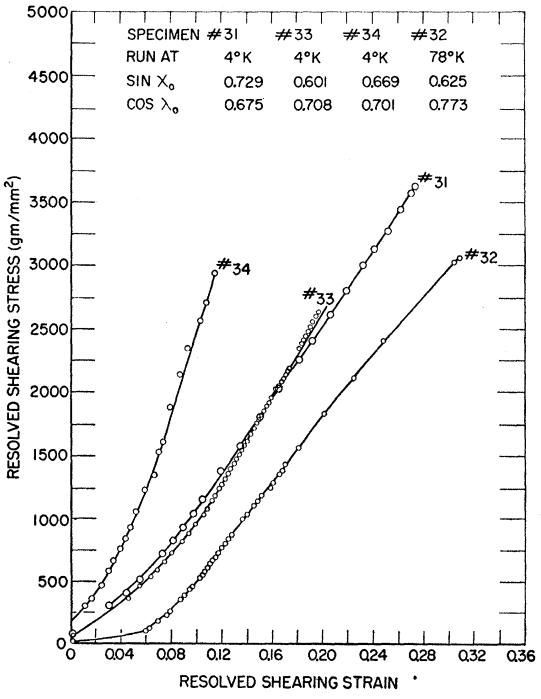

FIG. 3. Stress-strain curves. Note that the slope of specimen No. 34 is higher than those of No. 31 and No. 33 demonstrating the orientation dependence of the curve. Also note that the slope of No. 32 in the rising portion is comparable with those of similarly oriented specimens tested at helium temperature.

(3) The resolved stress strain curve at helium temperature is linear (up to 15% extension). Curves obtained at 78°K and above are parabolic.

(4) There exists an orientation dependence of the resolved stress-strain curve (i.e., the slope of the stress-strain curve increases by a factor of two in going from the center of the stereographic triangle towards the corners which give multiple slip).

The annealing behavior is characterized by the following features:

(1) The resistivity change introduced by deformation at helium temperature showed some annealing at 78°K (i.e., about 10% of $\Delta\rho$ annealed out).

(2) About 55% of the total increase anneals out in the range 150°K to 300°K. This annealing begins at 190°K for specimens having 5 to 10% extension and at 150°K for specimens having 15 to 20% extension.

(3) Crystals extended at 4°K show an upper yield point on further extension at the low temperature after warming to 300°K (see Fig. 6). In some cases, this upper yield point can be developed by aging at 78°K.

(4) Crystals extended at 4°K and 78°K show appreciable annealing of the stress necessary for further deformation at the low temperature after warming to 300°K. This is of course after the upper yield stress has been exceeded (see Figs. 4 and 6).

5. DISCUSSION

The data reported here for aluminum together with that of Blewitt and co-workers on copper suggest that: (1) the resolved stress-strain curve for any face-centered metal is linear at sufficiently low temperatures; (2) aluminum and copper differ considerably in their temperature scales. For example aluminum at 78°K resembles copper at some temperature above 300°K.

The observed isotropy can be understood either by: (1) supposing that the resistivity introduced by dislocations is negligible in comparison with that introduced by the lattice vacancies and interstitials, or by: (2) assuming that although macroscopically single slip occurs, on a microscopic view dislocations are introduced on many slip systems so that isotropy results.

[4] T. H. Blewitt (to be published); Blewitt, Coltman, and Redman, *Bristol Conference on Defects in Solids* (The Physical Society, London, 1955), p. 369.

Some support for the first alternative can be obtained by comparing Hunter and Nabarro's[5] dislocation calculation with Jongenberger's[6] calculation for vacancies. If one assumes that equal numbers of edge and screw dislocations are produced, then a vacancy is about 16 times as effective in producing resistivity as is one atomic length of dislocation.

It is possible that an x-ray method can be devised to decide this question since, if only one slip system acts, then the atomic displacements produced by the dislocations would be in the active slip direction. A result of this would be that the Bragg reflections from a few particular crystallographic planes would not be broadened. If, on the other hand, many slip systems produce dislocations, all of the Bragg reflections would be broadened.

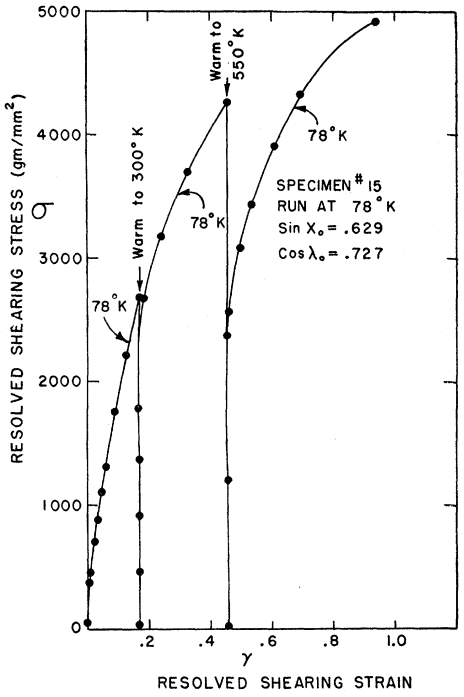

FIG. 4. Stress-strain curve at nitrogen temperature. Note that warming to 300°K produces measurable softening.

The fact that an upper yield point is produced in both aluminum and copper on appropriate aging suggests that these materials contain extended dislocations. The reasoning is as follows: If we assume that the phenomenon is not associated with impurities, then vacancies and interstitials would produce jogs in complete edge-type dislocations. Such jogs would probably not restrict their glide appreciably. However, an interstitial or a vacancy would not completely relieve the local strain if it is located at one of the half-dislocations of an extended dislocation. If then an applied stress tends to move the half-dislocation, it can separate the dislocation and the point imperfection. Thus, in the case of a whole dislocation, the point imperfection tends to disappear, to become a part of the dislocation, and to move with it; whereas in the case of the extended dislocation the point imperfection probably retains its identity and behaves more like an impurity atom.

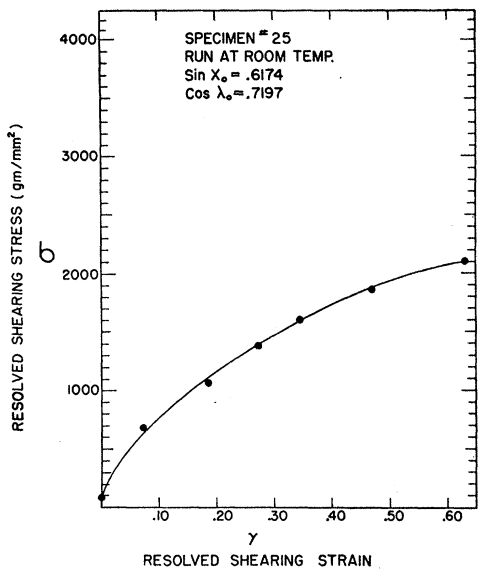

FIG. 5. Stress-strain curve at room temperature.

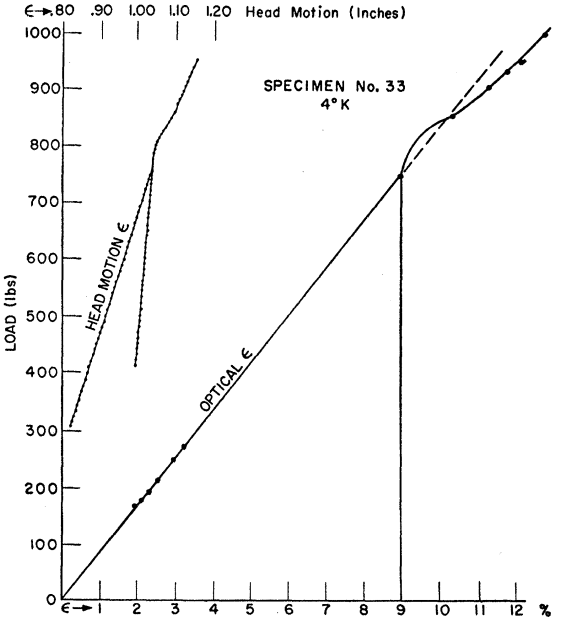

FIG. 6. Aging and softening of crystal produced by annealing at 300°K between strainings at 4°K. The extensions given in the upper curve were measured by the motion of the upper head of the tensile machine; those given in the lower curve were measured on the specimen by an optical comparator.

[5] S. C. Hunter and F. R. N. Nabarro, Proc. Roy. Soc. (London) **A220**, 542 (1953).

[6] P. Jongenburger, Phys. Rev. **90**, 710 (1953).

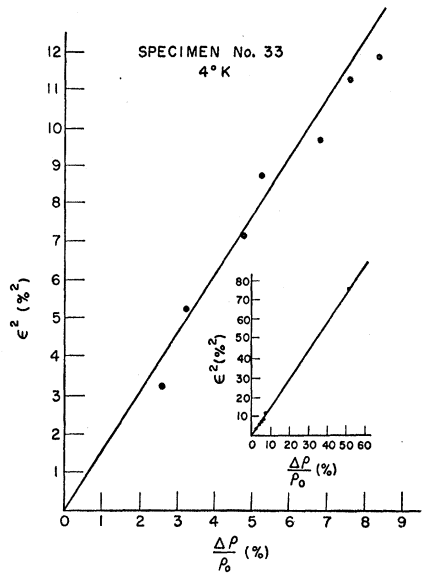

FIG. 7. Plot showing that the increase in the resistivity on deformation at 4°K is proportional to the square of the resolved shearing strain.

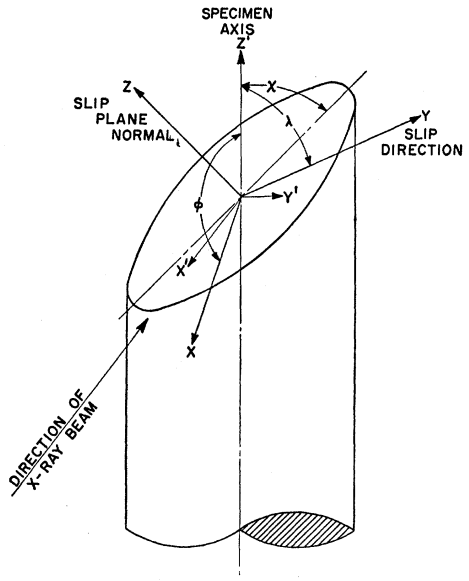

FIG. 8. The crystal orientation.

A more complete discussion will follow in a later paper.

APPENDIX I

The expression for the potential difference between two points on the specimen presented in the test is given in terms of the distances between points in the slip system. In practice, the positions of the potential probes relative to this coordinate system are not immediately known. Furthermore, although the angles for the crystal prior to deformation involved in the above expression may be obtained directly from a Laue back-reflection photograph, the values of these angles change as deformation proceeds.

To obtain these quantities, we use a laboratory system of reference. The coordinate axes of this system are defined by the specimen axis, taken as the z'-axis, and two other orthogonal directions. It is convenient to choose these as the direction of incidence of the x-ray beam when taking a Laue photograph (x') and the third orthogonal direction (y'). With this choice of axes, all the potential leads at the beginning of the experiment lie either on the x'-axis or the y'-axis. The two pertinent systems are shown in Fig. 8.

The positions of the potential probes in the slip system prior to deformation are then obtained by writing down the positions in laboratory system and transforming to the slip system by use of a rotation matrix obtained from examination of the Laue photograph. To obtain the positions after deformation as well as the required angles, we proceed as follows.

Let the quantities before deformation have the subscript 0; following deformation, ϵ. Since the deformation is a pure shear in the direction y of a magnitude a, each point $P_0(x_0,y_0,z_0)$ transforms into the point $P(x_\epsilon,y_\epsilon,z_\epsilon)$ by glide in the y-direction. Thus, the transformation is

$$x=x_0, \quad y=y_0+az_0, \quad z=z_0.$$

Also, for the line elements of P_0 and P_ϵ, we have

$$L_0^2=x_0^2+y_0^2+z_0^2, \quad L_\epsilon^2=x_\epsilon^2+y_\epsilon^2+z_\epsilon^2,$$
$$y_0=L_0\cos\lambda_0, \qquad y_\epsilon=L_\epsilon\cos\lambda_\epsilon,$$
$$z_0=L_0\sin\chi_0, \qquad z_\epsilon=L_\epsilon\sin\chi_\epsilon.$$

By combining equations, it follows that

$$(L_\epsilon/L_0)^2=(L_0^2+2ay_0z_0+a^2z_0^2)/L_0^2$$
$$=1+2a\sin\chi_0\cos\lambda_0+a^2\sin^2\chi_0.$$

Solving for a,

$$a=\frac{1}{\sin\chi_0}\{[\epsilon^2-\sin^2\lambda_0]^{\frac{1}{2}}-\cos\lambda_0\},$$

where $\epsilon=L_\epsilon/L_0$. In a better form for computation,

$$a=(\cos\lambda_\epsilon/\sin\chi_\epsilon)-(\cos\lambda_0/\sin\chi_0).$$

From the diagram, it is obvious that $L_0\sin\lambda_0=L_\epsilon\sin\lambda_\epsilon$ and since $z_\epsilon=z_0$, $L_\epsilon\sin\chi_\epsilon=L_0\sin\chi_0$, we have

$$\epsilon=L_\epsilon/L_0=\sin\lambda_0/\sin\lambda_\epsilon=\sin\chi_0/\sin\chi_\epsilon.$$

In terms of the notation used above, the potential distribution is given by

$$\Delta\varphi=(I/A)[\rho_x\Delta x\cos\varphi+\rho_y\Delta y\cos\lambda+\rho_z\Delta_z\sin\chi].$$

The above expression was used for each set of potential probes. From the initially known separation and Laue picture, the distances, area, and angles involved were determined. These quantities were then calculated again for each level of strain at which voltage and current measurements were made. Thus, an expression was obtained for each set of probes used involving three

unknowns—the three components of resistivity. In principle, three such measurements were then sufficient; in practice, several more were made and a least-squares method used to actually compute the components.

APPENDIX II

The analysis of the data presents one peculiar difficulty. It will be noted that the contribution of a resistivity component to the actual resistance reading is weighted with a cosine dependence as well as a component of the lead separation. Since current is passed axially through the specimen, it is an unfortunate fact that $\cos(xz')$ is always much smaller than the other cosines. The x-direction is always close to the horizontal for a vertical current flow. To aggravate the matter, $\cos(xz')$ becomes smaller with slip. This has the effect of introducing a large amount of error in ρ_x.

To minimize this error, an attempt was made to choose crystals with orientations having as large a value of $\cos(xz')$ as possible, as well as representing crystals which remained well out of the double-slip region of the unit stereographic triangle. For this reason, $\cos(yz')$ $\cong\cos(zz')\cong 0.7$. It is easy to see that the results listed in Table II for specimen 33, which represents an almost ideal orientation in these respects, are much more consistent than the others in its values of ρ_x; the results listed in Table III for specimen 32, which represents a poor orientation in these respects, are probably not reliable in values of ρ_x. The values of ρ_x must be regarded as the most poorly determined experimental quantity.

Another source of error is the deviation of the potential probes from the positions intended. To minimize this error, resistance measurements were made before extension and the positions corrected to agree with these measurements. In no case did the adjustment exceed the probe diameter. Following elongation, the calculated new positions of the leads were compared with those observed in a microscope. The agreement was better than 2%, which confirms the geometrical analysis used.

It is believed that a fair estimate of accuracy seems to be about 10% for strains less than 6% to 5% for larger strains. This is the case for ρ_y and ρ_z. In the case of ρ_x the corresponding errors were 50% and 20%.

PHYSICAL REVIEW VOLUME 101, NUMBER 3 FEBRUARY 1, 1956

Structure Sensitivity of the X-Ray Coloration of NaCl Crystals*

R. B. GORDON† AND A. S. NOWICK
Hammond Metallurgical Laboratory, Yale University, New Haven, Connecticut
(Received October 24, 1955)

Room temperature measurements of the rate of coloring of NaCl crystals by x-rays at different depths below the irradiated surface and for different states of deformation and heat treatment are reported. From the results it is concluded that two mechanisms of coloring operate in these crystals. The first, or "rapid-type" coloring, approaches a saturation density of F-centers of the order of $10^{17}/cm^3$, and appears to result from the generation of color centers from vacancies already present in the unirradiated crystal. The second, or "slow-type" coloring, takes place at a constant rate until F-centers in excess of $10^{18}/cm^3$ are formed. This type of coloring, which is usually observed only near the irradiated surface, is due to the generation of F-centers at dislocations, and is responsible for the hardness and density changes produced by the x-rays. Rapid-type coloring is found to occur at essentially the same rate in deformed crystals and in carefully annealed crystals; recovery at low temperatures after deformation, however, decreases the colorability. These results indicate that the principal effects of deformation and heat treatment on colorability may be related to the state of dispersion of impurities.

I. INTRODUCTION

IT is now well known that the principal center responsible for the coloration observed in alkali halide crystals after exposure to ionizing radiations (the F-center) consists of a negative ion vacancy which has trapped an electron. It is to be expected, then, that the rate at which F-centers form in a crystal subjected to irradiation (the "darkenability" or "colorability") will be a structure sensitive property. Seitz[1] has in fact suggested that since vacancies may be generated during plastic flow, the colorability of deformed crystals should be enhanced compared to that of annealed crystals. Another reason for anticipating increased colorability in deformed crystals is that F-centers can be generated at dislocations[2]; a deformed crystal should contain many more such sources for F-centers than a well-annealed crystal.

Experimental evidence pertaining to the effect of plastic deformation on darkenability is very inadequate. Much of the work in this field was carried out prior to 1930 by Smekal[3] and by Przibram.[4] In the case of rock salt irradiated with γ rays, Przibram found that a

* This research was supported by the U. S. Air Force through the Office of Scientific Research of the Air Research and Development Command.

† Now at School of Mines, Columbia University, New York, New York.

[1] F. Seitz, Phys. Rev. **80**, 239 (1950).

[2] F. Seitz, Revs. Modern Phys. **26**, 7 (1954).

[3] A. Smekal, Z. Ver. deut. Ing. **72**, 667 (1928).

[4] K. Przibram, Z. Physik **41**, 833 (1927); Wein. Ber. (IIa) **136** 43 (1927).